Photovoltaic Material Characterization With Steady State and Transient Photoluminescence

Xufeng Wang, Jayprakash Bhosale, James Moore, Rehan Kapadia, Peter Bermel, Ali Javey, and Mark Lundstrom

***Abstract*—In this study, we develop an approach to characterize the surface and bulk properties for thin films of photovoltaic materials by combining two experimental photoluminescence (PL) techniques with one multiphysics simulation. This contactless, in-line characterization technique allows reliable extraction of key lifetime parameters. In this study, we first discuss the strengths and weaknesses of both steady-state and transient PL techniques (specifically, steady-state PL excitation spectroscopy and time-resolved PL) and show that combining them with numerical simulation can be used to extract surface and bulk lifetimes self consistently. The method is applied to InP thin films grown with a novel vapor–liquid–solid method. The InP thin film tested is found to have a bulk Shockley–Read–Hall (SRH) lifetime of 12 ns and a front surface recombination velocity of 5×10^4 cm/s.**

***Index Terms*—Charge carrier lifetime, indium phosphide, photoluminescence (PL), photovoltaic cells.**

I. Introduction

VARIOUS characterization techniques based on photoluminescence (PL) of semiconductors offer powerful insights into the properties of photovoltaic materials that affect solar cell performance. In particular, the transient form of PL, namely the time-resolved photoluminescence (TRPL) method has been widely used in material lifetime characterization [1]–[7]. In a TRPL setup, the sample is excited with a short laser pulse. The generated carriers move within the sample and eventually recombine [8]. The resulting radiative emission versus time plot serves as an indirect probe of the characteristic sample lifetimes. Compared with transient PL, steady-state PL techniques such as PL excitation spectroscopy (PLE) are far less widely used [9], [10]. In the PLE technique, a constant monochromatic light source is used to excite the sample, and the radiative emission flux from the sample is recorded. The flux ratio between the emission and source yields the external fluorescence efficiency [11]

$$\mathrm{PLE}(\lambda_{\mathrm{in}}) = \frac{\phi_{\mathrm{emit}}}{\phi_{\mathrm{in}}(\lambda_{\mathrm{in}})} \tag{1}$$

where ϕ_{in} is the incident photon flux at wavelength λ_{in}, and ϕ_{emit} is the radiative emission from the sample.

By varying the incident light wavelength, the external fluorescence efficiency is measured as a function of excitation wavelength. Although PLE does not yield lifetime directly as TRPL does, the external fluorescence efficiency measures the gap between a solar cell and its ultimate radiative efficiency limit. It has, therefore, been suggested as an effective contactless method for inline quality control of solar cells [12]–[14].

PL-based characterization is important and widely used, but also challenging to interpret when applied to materials with novel compositions or growth methods. In such cases, the PL data usually do not always follow simple analytical models [15]–[18]. For example, it has been shown that the presence of a junction or surface band-bending can lead to a false observation of significantly larger lifetime in a TRPL measurement [5], [19]. Moreover, traditional TRPL is limited by the strong absorption near the sample surface, according to Beer's law. Novel and complex techniques, such as the two-photon excitation method must be applied to remedy this shortcoming [20]–[22]. Thus, an analytical parameter fit is often insufficient to capture the many uncertainties and subtleties in material properties (e.g., lifetime parameters). Therefore, a general and robust method is needed beyond the simple analytical interpretation of the PL data to characterize the various novel photovoltaic materials being developed today.

In this study, using a combination of TRPL and PLE coupled with rigorous numerical simulation, we show that the surface and bulk recombination lifetime can be quantitatively extracted for an arbitrary photovoltaic material. Our experimental and numerical methods are discussed in Section II. In Section III, we investigate the differing sensitivities of TRPL and PLE to surface and bulk recombination, which explains our reasons to couple the TRPL and PLE approaches. We then apply our proposed method to evaluate an InP substrate sample and a VLS-grown InP sample in Section IV. Our conclusions are summarized in Section V.

II. Method

A. Experimental Setup

The PLE measurements of thin-film samples involve measuring an extremely weak PL signal often accompanied by a large scattered radiation background, due to the rough surface topography of many thin films. In order to address these issues,

Manuscript received July 10, 2014; revised September 9, 2014; accepted September 22, 2014. Date of publication October 16, 2014; date of current version December 18, 2014. This work was supported by the Department of Energyy (DOE), under DOE Cooperative Agreement DE-EE0004946 ("PVMI Bay Area PV Consortium"), and the Semiconductor Research Corporation, under Research Task 2110.003 ("Network for Photovoltaic Technologies").

X. Wang, J. Bhosale, J. Moore, P. Bermel, and M. Lundstrom are with the School of Electrical and Computer Engineering, Purdue University, West Lafayette, IN 47907 USA (e-mail: wang159@purdue.edu; jbhosale@purdue.edu; moore32@purdue.edu; pbermel@purdue.edu; lundstro@ecn.purdue.edu).

R. Kapadia and A. Javey are with the Department of Electrical Engineering and Computer Science, University of California, Berkeley, CA 94720 USA, and also with the Material Science Division, Lawrence Berkeley National Laboratory, Berkeley, CA 94720 USA (e-mail: rkapadia@eecs.berkeley.edu; ajavey@eecs.berkeley.edu).

Color versions of one or more of the figures in this paper are available online at http://ieeexplore.ieee.org.

Digital Object Identifier 10.1109/JPHOTOV.2014.2361015

2156-3381 © 2014 IEEE. Personal use is permitted, but republication/redistribution requires IEEE permission.
See http://www.ieee.org/publications_standards/publications/rights/index.html for more information.

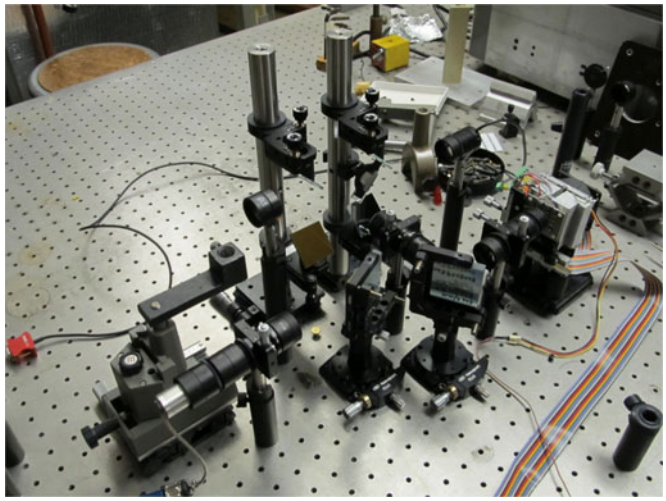

Fig. 1. PLE setup used in this study. Several electrical components, including the LED driver unit, lock-in amplifier, and controlling PC, are not captured in this picture.

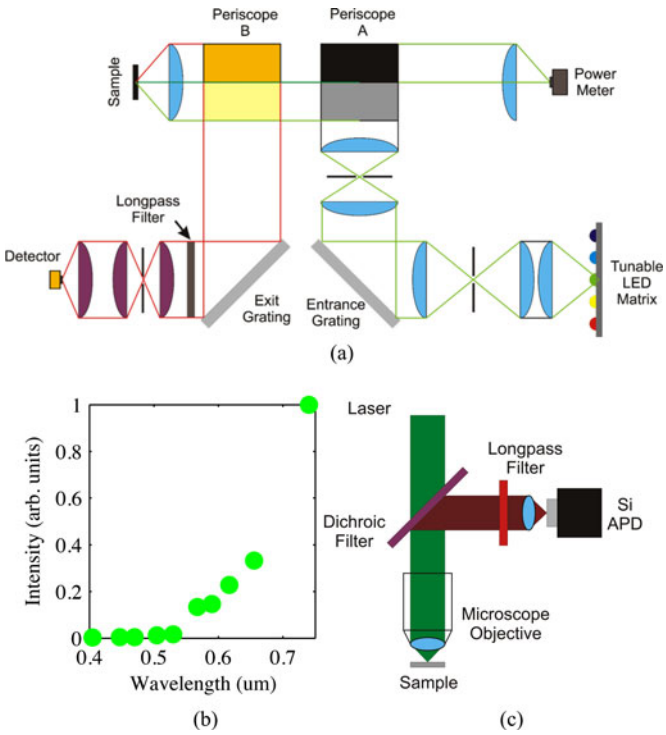

Fig. 2. (a) Layout for the PLE experimental setup used in this study. The measurement event starts at the tunable LED matrix at the lower right corner. The sample under testing is at the upper left corner, and the PLE emission signal is detected at the lower left corner. (b) PLE for an unpassivated GaAs wafer. (c) TCSPC TRPL experimental setup used in this study.

the PLE measurements are performed with an LED-based setup as shown in Figs. 1 and 2(a). In this setup, a tunable LED source [23] provides a bright light output, which is then collimated and focused onto the entrance grating in order to tune the bandwidth of the source (∼15 nm) near the peak intensity wavelengths. This light is then split into two components with a beam splitter, where one part is used to monitor the incident photon flux and the other part is focused on the sample. PL excited by the incident light is then collimated and focused onto the exit grating, which is positioned to select the band-edge PL radiation while rejecting the incident light scattered from the sample. The PL signal is then passed through a long pass filter to further ensure the incident light rejection. Finally, the PL is focused on a Si photodiode detector connected to a lock-in amplifier. The silicon photodiode, in reverse bias, multiplies the photon-excited free carriers through impact ionization. It has a high gain, which is defined as the charge multiplication factor per photon-excited carrier. The modulation in the LED light intensity required for the lock-in detection is achieved by driving the LED with an ac signal controlled by the lock-in amplifier. Details regarding the instrumentation setup and calibration will be published elsewhere.

Although we measured InP samples in this study, this PLE setup can be applied to other materials. In Fig. 2(b), the PLE setup has been used to measure an unpassivated GaAs wafer, where strong suppression of the PLE signal at short wavelength region is observed. This is likely due to the unpassivated GaAs wafer having a very high surface recombination. In addition, a higher quality GaAs thin-film double-hetero structure has also been investigated using this PLE setup [10].

The TRPL measurements were conducted using a standard confocal microscope-based time-correlated single photon counting (TCSPC) setup [24] shown in Fig. 2(c). In this setup, a 550-nm-pulsed laser is focused on the sample with a microscope objective. The PL collected by the objective is then passed through a dichroic filter to reject the laser light from the PL radiation. A long-pass filter further ensures reliable PL signal for detection. The PL photons are detected with a Si avalanche photo diode in order to perform the time-correlated photon counting.

B. Simulation Setup

Since the techniques used here are both based on PL, a correct model of PL emission is critical for proper analysis of the results. A simple integration of radiative recombination as emission, as commonly seen in the literature, can be inaccurate and inadequate due to the structural dependence of emission caused by photon recycling. Instead, we opt to 1) calculate a structure-independent intrinsic radiative recombination rate and 2) use ray-tracing to calculate the amount of radiative emission that is reabsorbed (recycled) or that escapes as the PL signal. The approach is similar to the one used by Durbin *et al.* [25], [26].

Radiative recombination is an intrinsic property of semiconductor material at a finite temperature, and it is related to the absorption coefficient by the Roosbroeck–Shockley equation [27], [28]

$$R_{\text{emit}}(V=0) = \int_0^\infty R_{\text{emit}}(v)dv = \int_0^\infty \frac{8\pi \mathrm{v}^2 n^2}{c^2} \frac{\alpha(v)}{e^{hv/kT}-1} dv \quad (2)$$

where $\alpha(v)$ is the optical absorption coefficient at frequency v, and n is the index of refraction. The condition $V = 0$ indicates this equation is valid at equilibrium. Away from equilibrium,

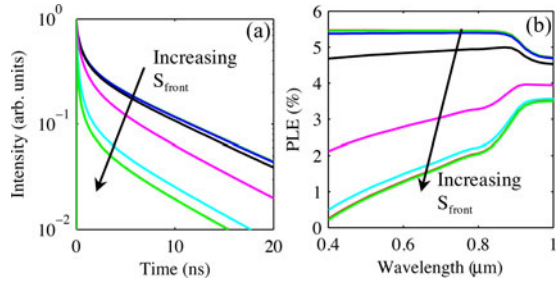

Fig. 3. Numerical simulations demonstrate that (a) TRPL and (b) PLE show greatly differing responses to variations in surface recombination velocity over the range $S_{\rm front}$ = 1, 10, 10^2, 10^3, 10^4, 10^5, 10^6, and 10^7 cm/s at $\tau_{\rm SRH}$ = 28 ns. ($S_{\rm front}$ = 1, 10, 10^2, and 10^3 cm/s curves are very close to each other.) PLE-based estimates of $S_{\rm front}$ generally have much smaller errors.

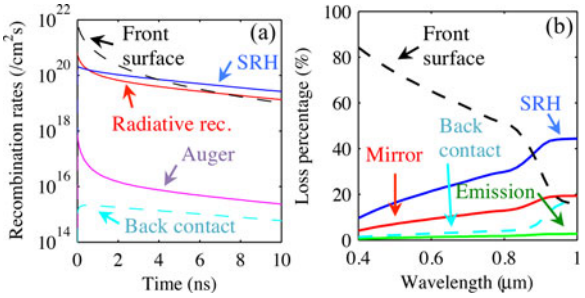

Fig. 4. Internal loss components predicted for (a) TRPL versus time and (b) PLE versus wavelength at $S_{\rm front} = 5 \times 10^4$ cm/s and $\tau_{\rm SRH} = 12$ ns. These specific parameters are chosen since they provide the best overall fit to the InP sample tested, as shown in Fig. 7.

the quasi-Fermi levels split so that

$$R_{\rm emit}(V) = R_{\rm emit}(V=0)e^{qV/kT}. \tag{3}$$

Based on this idea, we upgraded an existing electro-optically coupled simulation framework based on Sentaurus to simulate PL-based characterization [29]. As a result, the photon recycling is taken into account and the various radiative loss components are resolved. For more details on this electro-optically coupled simulation framework, readers are referred to [29] and [30], where this framework has been successfully used to investigate single-junction GaAs solar cells and nanowire solar cells.

III. Time-Resolved Photoluminescence and Photoluminescence Excitation Spectroscopy Sensitivity

Although both TRPL and PLE measurements are influenced by surface and bulk recombination, their sensitivities to each mechanism vary. To illustrate this idea, we simulate and compare the TRPL and PLE for a 3-μm-thick InP thin film. Fig. 3(a) shows the TRPL with 28-ns bulk Shockley–Read–Hall (SRH) lifetime ($\tau_{\rm SRH}$) for various front surface recombination velocities ($S_{\rm front}$). The surface only affects the PL decay rate during the first few nanoseconds. Using $S_{\rm front} = 5 \times 10^4$ cm/s and $\tau_{\rm SRH} = 12$ ns, for example, the time-dependent recombination rates are shown in Fig. 4(a). During the initial few nanoseconds,

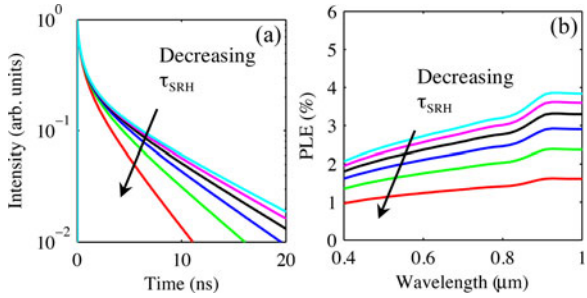

Fig. 5. (a) TRPL and (b) PLE for $\tau_{\rm SRH}$ = 5, 9, 13, 17, 21, and 25 ns at $S_{\rm front} = 10^4$ cm/s.

the newly generated electron–hole pairs have not yet diffused far away from the front surface; therefore, front surface recombination dominates the PL decay. As the carriers diffuse toward the back, most of the recombination occurs in the bulk, and the decay rate becomes dominated by the bulk SRH lifetime. Ideally, $S_{\rm front}$ can be extracted by a double-exponential fit to the TRPL data, but it is often not feasible in practice due to factors such as injection level and carrier mobility, or experimental factors such as instrument response time. As a result, TRPL-based estimates of surface recombination velocity have significant uncertainty.

In contrast to TRPL, PLE displays a clear and predictable dependence on $S_{\rm front}$ in Fig. 3(b). Due to the change of absorption coefficient, the generation profile of carriers varies across different wavelengths. Fig. 4(b) displays the recombination components versus wavelength for $S_{\rm front} = 5 \times 10^4$ cm/s. As the centroid of generation moves away from the front surface, the impact of front surface recombination decreases, and the external fluorescence efficiency increases as a result.

Because of these effects, PLE can be interpreted as an "open-circuit" version of the external quantum efficiency (EQE) measurement [13]. Both PLE and EQE are steady-state measurements using incident light sources as a function of wavelengths. Instead of detecting the short-circuit current as in EQE, PLE measures the radiative emission under open-circuit condition. The presence of surface recombination decreases the current collected in EQE, and in the case of PLE, it decreases the amount of free carriers recombining radiatively. In fact, it has been shown that, in a high quality sample, the EQE and PLE are closely related [10].

Consider next the sensitivity of these techniques to bulk lifetime. For a fixed $S_{\rm front} = 10^4$ cm/s, both TRPL and PLE display sensitivity to a change in the bulk SRH lifetime, as shown in Fig. 5(a) and (b), respectively. In practice, however, the variation in PLE observed in Fig. 5(b) may be difficult to observe, since the absolute measurement of PLE can be difficult, and less than 1% difference in values can easily be washed out by noise.

To summarize, TRPL is more sensitive to bulk properties, particularly when the surface is well passivated, while the extraction of surface information is much more robust in PLE. The two techniques nicely compliment each other, and both involve complicated internal physics that require electro-optically coupled simulation to self-consistently resolve.

Fig. 6. Overall structure for the two samples investigated in this study. (a) VLS-grown InP thin film on top of a Molybdenum substrate and (b) InP wafer that is 250 μm thick.

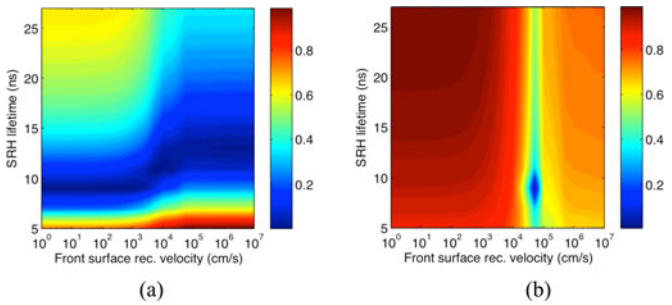

Fig. 7. VLS-grown InP thin film: least-square error map as a function of SRH lifetime and front surface recombination velocity when fitting to simulations of (a) TRPL and (b) PLE. The least-square error units are arbitrary, with cold blue regions indicating smaller error and best fit and with hot red regions being the opposite.

IV. Results and Analysis

A. Vapor–Liquid–Solid-Grown InP Thin Film

Recently, InP thin films have been grown via a novel VLS growth method [31]. The large grain size and good uniformity make it a promising technique for low-cost InP thin-film photovoltaics. In this section, the proposed TRPL and PLE coupled approach is applied to these InP thin films in order to derive quantitative information regarding surface and bulk recombination. The structure of the VLS-grown InP thin-film sample is shown in Fig. 6(a).

TRPL and PLE for various $S_{\rm front}$ and SRH lifetimes are simulated using the electro-optically coupled simulator, and compared with the measured curves. The maps of least-square fitting errors for TRPL and PLE as a function of SRH bulk lifetime and surface recombination velocity $S_{\rm front}$ are displayed in Fig. 7(a) and (b), respectively. The heightened sensitivity of TRPL to bulk properties, and PLE to surface properties, can be clearly seen as stronger gradients in those directions. By minimizing the overall error between both of our measurements and simulations, we find $S_{\rm front} = 5 \times 10^4$ cm/s and $\tau_{\rm SRH} = 12$ ns represents our best estimate of the overall material properties. While the precision of this estimate of each property is fairly good, to several percent, estimating the absolute accuracy would require an independent measurement such as the two-photon TRPL technique [21], [22].

Fig. 8(a) and (b), respectively, shows the simulated TRPL and PLE curve for the estimated material parameters compared with the measured data. Both display a good overall match. The only deviation is in TRPL within the first two nanoseconds, when the surface recombination dominates. In practice, TRPL curves often do not display such sharp features due to lagged instrument response artificially prolonging the delay and adding noise. A convolution of simulated TRPL with the instrument response function (IRF) should further improve agreement over the first few nanoseconds. For our TRPL setup, the IRF has significant effect on the first two nanoseconds of the TRPL measurement [32]. When fitting the TRPL data, the data within the first two nanoseconds are thus discarded.

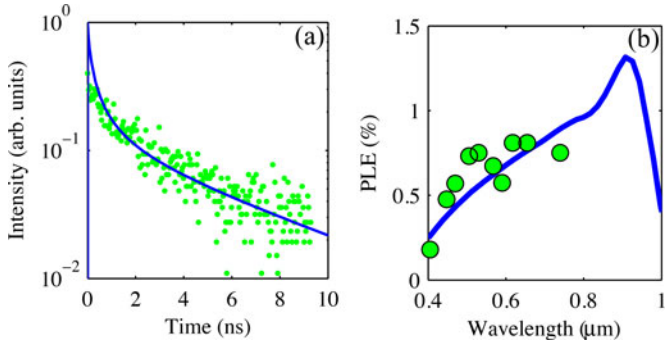

Fig. 8. Best overall fit for (a) TRPL and (b) PLE. Simulations are solid blue curves, and measurements are green dots. The measurements displayed are from one set of TRPL and PLE, respectively. The PLE measurement is reproducible, and with the use of a lock-in amplifier coupled with the LED sources, each data point in the PLE is the average of a very stable set of readings taken from many successive measurements.

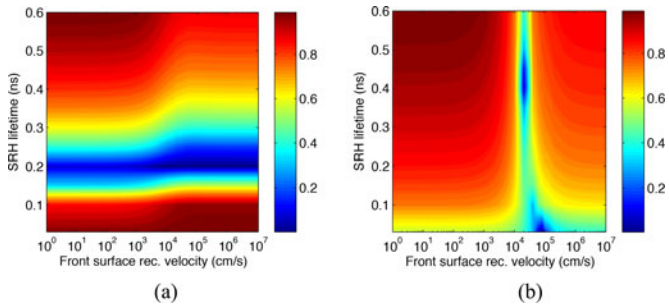

Fig. 9. InP wafer. Least square error map as a function of SRH lifetime and front surface recombination velocity when fitting to simulations of (a) TRPL and (b) PLE. The least-square error units are arbitrary, with cold blue regions indicating smaller error and best fit and with hot red regions being the opposite.

B. InP Substrate

For comparison, an n-type ($5 \times 10^{17}/{\rm cm}^3$) InP wafer of 250 μm thickness is also analyzed. The structure is shown in Fig. 6(b). The maps of least-square fitting errors for TRPL and PLE as a function of SRH bulk lifetime and surface recombination velocity $S_{\rm front}$ are displayed in–Fig. 9(a) and (b), respectively. Overall, $S_{\rm front} = 2 \times 10^4$ cm/s and $\tau_{\rm SRH} = 0.2$ ns give the best fitting for the InP wafer.

Compared with the VLS-grown InP thin-film sample, the wafer has significantly lower bulk SRH lifetime, which is expected in this sample. The bulk lifetime for the wafer is significantly lower, because it is lower quality, compared with the VLS-grown thin film. The surface recombination velocities and bulk lifetimes are also within the range of reported values in the

literature. In [33]–[36], the bulk InP lifetime can be as high as 500 ns. In this study, the VLS-grown thin film shows $\tau_{\mathrm{SRH}} = 12$ ns, which is expected due to the presence of grain boundaries. The wafer is known to have low material quality; therefore, the determined $\tau_{\mathrm{SRH}} = 0.2$ ns is also reasonable. The surface for the wafer is unpassivated in the same way as the VLS-grown InP thin film; thus, the derived surface recombination velocities are similar in both cases, which are $S_{\mathrm{front}} = 5 \times 10^4$ cm/s and $S_{\mathrm{front}} = 2 \times 10^4$ cm/s for the wafer and thin film, respectively. These are similar to the values reported in the literature [34], [37]–[39].

V. Conclusion

In this study, we demonstrated that combining TRPL and steady-state PLE experiments with multiphysics simulation techniques yields a precise contactless inline characterization method for photovoltaic materials. Differences in sensitivity to various loss mechanisms make TRPL and PLE more suitable for measuring bulk and surface recombination, respectively, particularly for not-so-well-passivated front surfaces. With a rigorous electro-optically coupled simulator properly modeling PL emission, we show quantitative bulk lifetime and surface recombination velocity can be extracted self-consistently. The method is applied to a novel VLS-grown InP thin film, and we find $S_{\mathrm{front}} = 5 \times 10^4$ cm/s and $\tau_{\mathrm{SRH}} = 12$ ns gives the best match between our simulation and experiments. The precision of the combined approach appears to be good, but the accuracy should be assessed using an independent measurement technique. We believe the method in this study is general enough to be applied to other materials and to be used as an inline method for quantitative process monitoring.

Acknowledgment

The authors would like to thank Dr. R. Ahrenkiel, Dr. D. Levi, and Dr. A. Kanevce of NREL for helpful discussions. They would also like to thank A. Ramdas of Purdue University for his support and lab access.

References

[1] R. K. Ahrenkiel, "Measurement of minority-carrier lifetime by time-resolved photoluminescence," *Solid-State Electron.*, vol. 35, pp. 239–250, Mar. 1992.

[2] D. K. Schroder, *Semiconductor Material and Device Characterization*, 3rd ed. New York, NY, USA: Wiley, 2006.

[3] W. K. Metzger, D. Albin, D. Levi, P. Sheldon, X. Li, B. M. Keyes *et al.*, "Time-resolved photoluminescence studies of CdTe solar cells," *J. Appl. Phys.*, vol. 94, p. 3549, 2003.

[4] W. K. Metzger, R. K. Ahrenkiel, and P. Dippo, "Time-resolved photoluminescence and photovoltaics," in *Proc. Dept. Energy Solar Energy Technol. Program Rev. Meeting*, 2004, pp. 1–2.

[5] R. K. Ahrenkiel, "Influence of junctions on photoluminescence decay in thin-film devices," *J. Appl. Phys.*, vol. 62, pp. 2937–2937, 1987.

[6] T. Trupke, B. Mitchell, J. W. Weber, W. McMillan, R. A. Bardos, and R. Kroeze, "Photoluminescence imaging for photovoltaic applications," *Energy Procedia*, vol. 15, pp. 135–146, 2012.

[7] T. Trupke and R. A. Bardos, "Photoluminescence: A surprisingly sensitive lifetime technique," in *Conf. Rec. 31st IEEE Photovoltaic Spec.*, 2005, pp. 903–906.

[8] A. Kanevce, D. H. Levi, and D. Kuciauskas, "The role of drift, diffusion, and recombination in time-resolved photoluminescence of CdTe solar cells determined through numerical simulation," *Progress Photovoltaics: Res. Appl.*, 2013.

[9] D. N. Hebert, J. A. N. T. Soares, and A. A. Rockett, "Photoluminescence and photoluminescence excitation spectroscopy of Cu(In,Ga)Se2 thin films," *MRS Proc.*, vol. 1165, pp. 1165-M03–1165-M05, 2011.

[10] D. Berdebes, J. Bhosale, K. H. Montgomery, X. Wang, A. K. Ramdas, J. M. Woodall *et al.*, "Photoluminescence excitation spectroscopy for in-line optical characterization of crystalline solar cells," *IEEE J. Photovoltaics*, vol. 3, no. 4, pp. 1342–1347, Oct. 2013.

[11] O. D. Miller, E. Yablonovitch, and S. R. Kurtz, "Strong internal and external luminescence as solar cells approach the Shockley–Queisser limit," *IEEE J. Photovoltaics*, vol. 2, no. 3, pp. 303–311, Jul. 2012.

[12] E. Yablonovitch, O. D. Miller, and S. R. Kurtz, "A great solar cell also needs to be a great LED: External fluorescence leads to new efficiency record," in *Proc. Nobel Symp. 153: Nanoscale Energy Converters*, 2013, pp. 9–11.

[13] M. A. Green, "Radiative efficiency of state-of-the-art photovoltaic cells," *Progress Photovoltaics: Res. Appl.*, vol. 20, pp. 472–476, 2012.

[14] S. Sandhu, Z. Yu, and S. Fan, "Detailed balance analysis and enhancement of open-circuit voltage in single-nanowire solar cells," *Nano Lett.*, vol. 14, pp. 1011–1015, Feb. 2014.

[15] D. Kuciauskas, A. Kanevce, J. N. Duenow, P. Dippo, M. Young, J. V. Li *et al.*, "Spectrally and time resolved photoluminescence analysis of the CdS/CdTe interface in thin-film photovoltaic solar cells," *Appl. Phys. Lett.*, vol. 102, p. 173902, 2013.

[16] D. Shvydka, V. G. Karpov, and A. D. Compaan, "Bias-dependent photoluminescence in CdTe photovoltaics," *Appl. Phys. Lett.*, vol. 80, p. 3114, 2002.

[17] H. W. Hillhouse and M. C. Beard, "Solar cells from colloidal nanocrystals: Fundamentals, materials, devices, and economics," *Current Opinion Colloid Interface Sci.*, vol. 14, pp. 245–259, 2009.

[18] A. P. Kirk, M. J. DiNezza, S. Liu, X.-H. Zhao, and Y.-H. Zhang, "CdTe versus GaAs solar cells: A modeling case study with preliminary experimental results," in *Proc. IEEE Photovoltaic Spec. Conf.*, 2013, pp. 2515–2517.

[19] D. A. R. Barkhouse, O. Gunawan, T. Gokmen, T. K. Todorov, and D. B. Mitzi, "Device characteristics of a 10.1% hydrazine-processed Cu2ZnSn(Se, S)4 solar cell," *Progress Photovoltaics: Res. Appl.*, vol. 20, pp. 6–11, 2012.

[20] A. Kanevce, D. Kuciauskas, T. A. Gessert, D. H. Levi, and D. S. Albin, "Impact of interface recombination on time resolved photoluminescence (TRPL) decays in CdTe solar cells," in *Proc. IEEE Photovoltaic Spec. Conf.*, 2011, pp. 000848–000853.

[21] D. Kuciauskas, A. Kanevce, J. M. Burst, J. N. Duenow, R. Dhere, D. S. Albin *et al.*, "Minority carrier lifetime analysis in the bulk of thin-film absorbers using subbandgap (two-photon) excitation," *IEEE J. Photovoltaics*, vol. 3, no. 4, pp. 1319–1324, Oct. 2013.

[22] E. S. Barnard, E. T. Hoke, S. T. Connor, J. R. Groves, T. Kuykendall, Z. Yan *et al.*, "Probing carrier lifetimes in photovoltaic materials using subsurface two-photon microscopy," *Sci. Rep.*, vol. 3, p. 2098, 2013.

[23] J. S. Bhosale, "High signal-to-noise Fourier transform spectroscopy with light emitting diode sources," *Rev. Sci. Instrum.*, vol. 82, pp. 093103–093103, 2011.

[24] L. A. Eldada, V. Buschmann, S. Fore, F. Koberling, A. Knigge, P. Kapusta *et al.*, "Characterization and quality control of semiconductor wafers using time-correlated single photon counting," *Proc. SPIE*, vol. 8470, p. 84700F, 2012.

[25] S. M. Durbin and J. L. Gray, "Numerical modeling of photon recycling in solar cells," *IEEE Trans. Electron. Devices*, vol. 41, no. 2, pp. 239–245, Feb. 1994.

[26] S. M. Durbin, J. L. Gray, R. K. Ahrenkiel, and D. H. Levi, "Numerical modeling of the influence of photon recycling on lifetime measurements," in *Proc. IEEE Phovoltaic Spec. Conf.*, 1993, pp. 628–632.

[27] W. Van Roosbroeck and W. Shockley, "Photon-radiative recombination of electrons and holes in germanium," *Phys. Rev.*, vol. 94, pp. 1558–1560, 1954.

[28] G. Lush and M. Lundstrom, "Thin film approaches for high-efficiency III-V cells," *Sol. cells*, vol. 30, pp. 337–344, 1991.

[29] X. Wang, M. R. Khan, J. L. Gray, M. A. Alam, and M. S. Lundstrom, "Design of GaAs solar cells operating close to the Shockley–Queisser limit," *IEEE J. Photovoltaics*, vol. 3, no. 2, pp. 737–744, Apr. 2013.

[30] X. Wang, M. R. Khan, M. Lundstrom, and P. Bermel, "Performance-limiting factors for GaAs-based single nanowire photovoltaics," *Opt. Exp.*, vol. 22, p. A344, 2014.

[31] R. Kapadia, Z. Yu, H.-H. H. Wang, M. Zheng, C. Battaglia, M. Hettick *et al.*, "A direct thin-film path towards low-cost large-area III-V photovoltaics," *Sci. Rep.*, vol. 3, p. 2275, 2013.

[32] "Investigating photocleavage using time-resolved emission spectra," 2014, Horiba Scientific, Time Resolved Fluorescence Applicat. Note TRFA-7.

[33] I. Tsimberova, Y. Rosenwaks, and M. Molotskii, "Minority carriers recombination in n-InP single crystals," *J. Appl. Phys.*, vol. 93, p. 9797, 2003.
[34] S. Bothra, S. Tyagi, S. K. Ghandhi, and J. M. Borrego, "Surface recombination velocity and lifetime in InP," *Solid-State Electron.*, vol. 34, pp. 47–50, 1991.
[35] G. A. Landis, P. Jenkins, and I. Weinberg, "Photoluminescence lifetime measurements in InP wafers," in *Proc. 3rd Int. Conf. Indium Phosphide Related Mater.*, 1991, pp. 636–639.
[36] A. Liu and Y. Rosenwaks, "Excess carriers lifetime in InP single crystals: Radiative versus nonradiative recombination," *J. Appl. Phys.*, vol. 86, p. 430, 1999.
[37] Y. Rosenwaks, Y. Shapira, and D. Huppert, "Evidence for low intrinsic surface-recombination velocity on p-type InP," *Phys. Rev. B*, vol. 44, pp. 13097–13100, 1991.
[38] Y. Rosenwaks, Y. Shapira, and D. Huppert, "Picosecond time-resolved luminescence studies of surface and bulk recombination processes in InP," *Phys. Rev. B*, vol. 45, pp. 9108–9119, 1992.
[39] H. C. Casey and E. Buehler, "Evidence for low surface recombination velocity on n-type InP," *Appl. Phys. Lett.*, vol. 30, p. 247, 1977.

Authors' photographs and biographies not available at the time of publication.